

Polarization of the microwave background in reionized models

Matias Zaldarriaga*

Department of Physics, MIT, Cambridge, Massachusetts 02139

(Received 12 August 1996)

I discuss the physics of polarization in models with early reionization. For sufficiently high optical depth to recombination the polarization is boosted on large scales while it is suppressed on smaller scales. New peaks appear in the polarization power spectrum; their position is proportional to the square root of the redshift at which the reionization occurs while their amplitude is proportional to the optical depth. For standard scenarios the rms degree of linear polarization as measured with a 7° full width at half maximum (FWHM) antenna (such as the one of the Brown University experiment) is $1.6 \mu\text{K}$, $1.2 \mu\text{K}$, $4.8 \times 10^{-2} \mu\text{K}$ for an optical depth of 1, 0.5, or 0, respectively. For a 1° FWHM antenna these same models give $2.7 \mu\text{K}$, $1.8 \mu\text{K}$, and $0.77 \mu\text{K}$. Detailed measurement of polarization on large angular scales could provide an accurate determination of the epoch of reionization, which cannot be obtained from temperature measurements alone.

[S0556-2821(97)04004-6]

PACS number(s): 98.70.Vc, 98.80.Es

I. INTRODUCTION

Since the first measurements of cosmic microwave background (CMB) anisotropies by the Cosmic Background Explorer (COBE) satellite a few years ago this field has seen a very rapid development. There have been a number of new detections on smaller angular scales [1,2] as well as a lot of progress on the theoretical side [3–5]. Proposed microwave background experiments may be able to measure cosmological parameters with great accuracy, although some of the parameters may be degenerate [3].

The polarization of the microwave background has also received attention. On the theoretical side the polarization induced by density perturbations in models with a standard ionization history has been studied both numerically [6] and analytically [7]. The possibility of using polarization to distinguish between scalar and tensor fluctuations has been investigated [8–10]. The temperature-polarization cross correlation function for tensor modes has also been studied as a possible probe of the importance of the tensor contribution to the CMB anisotropies [11]. More recently the possibility of using the CMBR polarization to measure primordial magnetic fields has been investigated [12].

On the experimental side, there have been a number of experiments [13–16]. An upper limit of 6×10^{-5} on the degree of linear polarization has been established. An experiment to measure CMB polarization is now under construction at Brown University.¹ It will measure the Q and U Stokes parameters using first a 7° full width at half maximum (FWHM) antenna and then a 1° one. The expected sensitivity of this instrument is of a few μK . The future satellite missions MAP and COBRAS/SAMBAS will also measure polarization [17,18].

It was soon realized that an early reionization of the universe will greatly enhance polarization [19]. The fact that in

universes that never recombined the polarization would also be large was noted in many of the above studies. More recently Ng and Ng [9] discussed the polarization generated in reionized universes with instantaneous recombination. The Sachs-Wolfe effect was the only source of anisotropies that they included. They concluded that reionization at a moderate redshift could boost polarization to the level of a few percent of the temperature perturbations. Although this conclusion is correct, to make detailed predictions for an experiment such as that being built at Brown a realistic recombination history should be used since polarization is very sensitive to the duration of recombination [7,20]. Baryons should also be included in the calculation as the acoustic oscillation in the photon-baryon plasma are very important to determine polarization.

In this paper I discuss in detail the physics behind the polarization generated in models where there was an early reionization after the usual recombination. These models show very distinct features in the polarization power spectrum including a new peak at low l . This peak is not present either in the standard recombination scenarios or in the cases where the universe never recombined and it is the cause of the boost in the polarization.

All the calculations were done using the code CMBFAST² recently developed by Uroš Seljak and the author [21]. This code is both fast and accurate so detailed predictions for the Brown experiment or future satellite missions such as MAP can be easily obtained.

II. STANDARD IONIZATION HISTORY

In this section I review previous results for the CMB polarization for a standard ionization history in a flat space-time. The anisotropy and polarization perturbations can be expanded in terms of Fourier modes, which are independent in the linear regime. For one mode with wave vector \vec{k} ,

*Electronic address: matiasz@arcturus.mit.edu

¹URL address: <http://www.physics.brown.edu/ObsCosmology/polarize/polarize.html> for details.

²This code is publically available, for a copy contact Uroš Seljak (useljak@cfa.harvard.edu) or the author.

$\Delta_T(\vec{k}, \vec{n})$ and $\Delta_P(\vec{k}, \vec{n})$ will denote the temperature and polarization perturbations, where \vec{n} is the direction of photon propagation. The perturbations can be further expanded in Legendre series,

$$\Delta(\vec{k}, \vec{n}) = \sum_l (2l+1)(-i)^l \Delta_l P_l(\mu), \quad (2.1)$$

where $\mu = \vec{k} \cdot \vec{n} / k$. This expansion applies both to the anisotropy and polarization perturbation [19,8,22].

The Boltzmann equations for the perturbations in the scalar case are given by [6]

$$\begin{aligned} \dot{\Delta}_T + ik\mu\Delta_T &= \dot{\phi} - ik\mu\psi \\ &+ \dot{\kappa} \left\{ -\Delta_T + \Delta_{T0} + i\mu v_b + \frac{1}{2} P_2(\mu)\Pi \right\}, \\ \dot{\Delta}_P + ik\mu\Delta_P &= \dot{\kappa} \left\{ -\Delta_P + \frac{1}{2} [1 - P_2(\mu)]\Pi \right\}, \\ \Pi &= \Delta_{T2} + \Delta_{P2} + \Delta_{P0}. \end{aligned} \quad (2.2)$$

Here the derivatives are taken with respect to the conformal time τ , and v_b is the velocity of baryons. The differential optical depth for Thomson scattering is denoted as $\dot{\kappa} = an_e x_e \sigma_T$, where $a(\tau)$ is the expansion factor normalized to unity today, n_e is the electron density, x_e is the ionization fraction, and σ_T is the Thomson cross section. The total optical depth at time τ is obtained by integrating $\dot{\kappa}$, $\kappa(\tau) = \int_\tau^{\tau_0} \dot{\kappa}(\tau) d\tau$. A useful variable is the visibility function $g(\tau) = \dot{\kappa} \exp(-\kappa)$. For a standard ionization history its peak defines the epoch of decoupling, when the dominant contribution to the CMB anisotropies arises.

These equations can be formally integrated to give ([21] and references therein),

$$\begin{aligned} \Delta_T &= \int_0^{\tau_0} d\tau e^{ik\mu(\tau-\tau_0)} e^{-\kappa} \\ &\times \left\{ \dot{\kappa} \left[\Delta_{T0} + i\mu v_b + \frac{1}{2} P_2(\mu)\Pi \right] + \dot{\phi} - ik\mu\psi \right\}, \\ \Delta_P &= -\frac{1}{2} \int_0^{\tau_0} d\tau e^{ik\mu(\tau-\tau_0)} e^{-\kappa} \dot{\kappa} \left[1 - P_2(\mu) \right] \Pi. \end{aligned} \quad (2.3)$$

Equation (2.3) is the basis for the line of sight approach used in CMBFAST.

The temperature anisotropy spectra, C_{Tl} is defined as

$$C_{Tl} = (4\pi)^2 \int k^2 dk P_\psi(k) |\Delta_{Tl}(k, \tau = \tau_0)|^2, \quad (2.4)$$

where $P_\psi(k)$ is the power spectrum of the metric perturbations.

The temperature angular correlation function is related to the temperature C_{Tl} power spectrum by

$$\begin{aligned} C(\theta) &= \langle \Delta T(\vec{n}_1) \Delta T(\vec{n}_2) \rangle_{\vec{n}_1 \cdot \vec{n}_2 = \cos\theta} \\ &= \frac{1}{4\pi} \sum_{l=0}^{\infty} (2l+1) C_{Tl} P_l(\cos\theta). \end{aligned} \quad (2.5)$$

Because the polarization in a tensor quantity the expressions for the correlation functions are somewhat more complicated. Polarization can be analyzed using spin-weighted spherical harmonics [23]; when considering the polarization produced by density perturbations only one power spectra C_{El} is enough to characterize polarization statistics:

$$\begin{aligned} C_{El}^{(S)} &= (4\pi)^2 \int k^2 dk P_\psi(k) [\Delta_{El}(k)]^2, \\ \Delta_{El}(k) &= \sqrt{\frac{(l+2)!}{(l-2)!}} \int_0^{\tau_0} d\tau S_E(k, \tau) j_l(x), \\ S_E(k, \tau) &= \frac{3g(\tau)\Pi(\tau, k)}{4x^2}, \end{aligned} \quad (2.6)$$

where j_l denote the spherical Bessel functions and $x = k(\tau_0 - \tau)$.

The root mean square fluctuations are given by

$$\langle P^2 \rangle \equiv \langle (Q^2 + U^2) \rangle = 2\langle Q^2 \rangle = \frac{1}{4\pi} \sum_{l=0}^{\infty} (2l+1) C_{El} W_l. \quad (2.7)$$

P is just the degree of linear polarization and W_l is the window function for the particular experiment under consideration.

Figure 1 shows the temperature and polarization C_l spectra obtained by numerically integrating the above equations using CMBFAST, for the standard cold dark matter (CDM) model ($\Omega_0 = 1$, $H_0 = 50 \text{ km sec}^{-1}$, and $\Omega_b = 0.05$), normalizing the result to the COBE measurement. Normalization was carried out using the fits to the shape and amplitude of the 4 yr COBE data described in [24], this approximately fixes $10 \times 11 \times C_{T10} / 2\pi \sim 830 \mu\text{K}^2$.

The features in the polarization power spectrum can be understood analytically [7]. Polarization is produced by Thomson scattering of anisotropic radiation. To be more precise, the source of polarization is the quadrupole of the intensity distribution in the rest frame of the electrons, Δ_{T2} in Eq. (2.2). Thus no polarization can be generated after decoupling if there is no reionization or anisotropy. Before recombination the photons and baryons were tightly coupled, the damping scale being only a few Mpc. For this reason the photon distribution function was nearly isotropic in the rest frame of the electrons and thus the generated polarization was extremely small. As photons and electrons decouple, the mean-free path of the photons starts to grow and temperature quadrupole moment is produced by free streaming. Now photons scattering off a given electron come from regions where electrons have slightly different velocities, i.e., the redshift of these photons and thus the intensity at a fixed wavelength depend on direction. The quadrupolar part of these temperature fluctuations is the source of the generated polarization. For wavelengths longer than the width of the last scattering surface $\Delta\tau_D$ the polarization perturbation can be shown to be [7]

$$\Delta_P = 0.51(1 - \mu^2) e^{ik\mu(\tau_D - \tau_0)} k \Delta\tau_D \Delta_{T1}(\tau_D). \quad (2.8)$$

τ_D is the conformal time of decoupling. Note that in the tight coupling regime $\Delta_{T1} \propto v_b$. The above formula shows that for

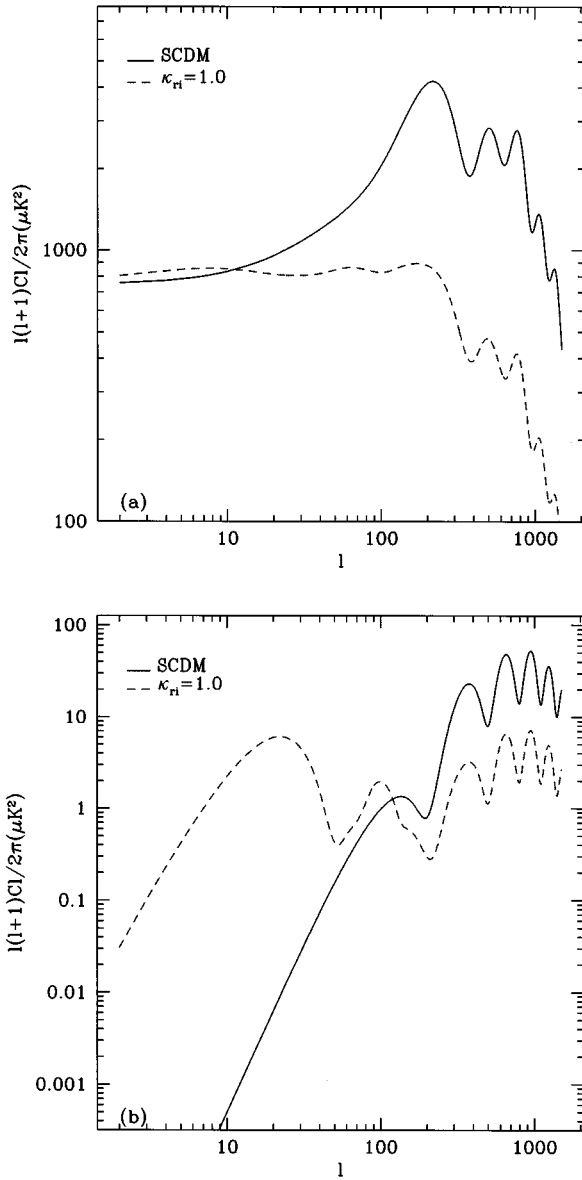


FIG. 1. $l(l+1)C_l/2\pi$ for both temperature (a) and polarization (b) for standard CDM and a model where the optical depth to recombination is $\kappa_{\text{ri}}=1.0$.

wavelengths longer than the width of the last scattering surface, polarization is proportional to the velocity difference between places separated by a distance $\Delta\tau_D$, the distance photons travel on average during decoupling.

For the standard adiabatic initial conditions $\Delta\tau_I$ and the baryon velocity vanish as $k\tau \rightarrow 0$ which together with the $k\Delta\tau_D$ factor in the previous expression explain the dramatic fall of polarization for large angular scales. For large wavelengths the quadrupole generated in the photon distribution as photons travel between their last scatterings is extremely small both due to the small distance they can travel compared to the wavelength as well as to the small velocity differences generated by these small \vec{k} perturbations.

For smaller angular scales, $l \geq 100$, the same acoustic oscillations that generate the Doppler peaks in the temperature anisotropy cause the peaks in the polarization spectrum. The peaks are located at different l values because they occur for different wave vectors. The anisotropy peaks correspond to

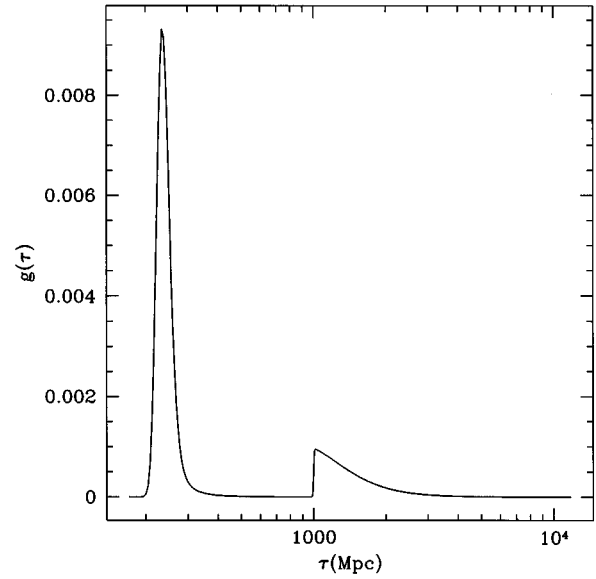


FIG. 2. Visibility function for standard CDM with reionization such that the optical depth to recombination is $\kappa_{\text{ri}}=1.0$.

the maxima of the temperature monopole [25,26,4] while from Eq. (2.8) those in the polarization occur at the maxima of the temperature dipole, i.e., the baryon velocity. In the tightly coupled regime, the temperature dipole is proportional to the time derivative of the monopole which explains the fact that polarization peaks occur at the l values where the temperature is at minima.

For smaller scales Silk damping damps the oscillations in the photon baryon plasma and this together with cancellations due to the finite width of the last scattering surface, is the cause for the decay in the C_l spectrum for both temperature and polarization (Fig. 1).

III. THE REIONIZED CASE

In this section I consider models with early reionization and try to explain the origin of the new features that appear in the polarization power spectrum. For definitiveness I use a standard CDM (SCDM) model where the universe reionized at an epoch such that the optical depth to recombination is κ_{ri} . This means for example that reionization occurred at a redshift of around $z_{\text{ri}} \sim 100$ if $\kappa_{\text{ri}}=1.0$. Figure 2 shows the visibility function, $g(\tau) = \dot{\kappa} \exp(-\kappa)$, for $\kappa_{\text{ri}}=1.0$ assuming that all hydrogen atoms are ionized up to the present epoch ($x_e=1.0$). The visibility function has a very simple interpretation, the probability that a photon reaching the observer last scattered between τ and $\tau+d\tau$ is just $g(\tau)d\tau$. The first peak in Fig. 2, occurring at $\tau \approx 120$ Mpc for SCDM ($h=0.5$) accounts for the photons that last scattered at recombination, the area under this peak, the probability that a photon came directly to us from this epoch, is $\exp(-\kappa_{\text{ri}})$. The area under the second peak gives the fraction of photons that scattered after reionization before reaching the observer, and is equal to $1 - \exp(-\kappa_{\text{ri}})$.

Figure 1 shows the result of numerically integrating the Boltzmann equations using CMBFAST for this reionized case. On small angular scales, the polarization ‘‘Doppler peaks’’ are suppressed, just as those in the anisotropy are. This is

very simple to understand, only a fraction $\exp(-\kappa_{\text{ri}})$ of the photons reaching the observer come from recombination, so their contribution to the C_l power spectrum is reduced by a factor $\exp(-2\kappa_{\text{ri}})$. On large angular scales new peaks appear in the polarization power spectrum. The temperature anisotropy shows no new peaks. This peaks are what boost the polarization on large scales and may take it to detectable levels.

Let us try to understand the origin of these peaks. For low values of k the largest perturbation in the photon distribution function is the monopole, Δ_{T0} because of the tight coupling between photons and electrons before recombination. Both the dipole and the quadrupole as well as the polarization perturbations are much smaller. But after photons and electrons decouple, all the temperature multipoles can grow by free streaming. Power is being carried from the zero multipole moment to higher ones, which is just a geometrical effect. The temperature quadrupole is growing by free streaming after recombination and so by the time of reionization there is an appreciable quadrupole that can generate polarization. The structure of this quadrupole explains the new features in the polarization power spectrum.

The formal line of sight solution for the polarization perturbation is

$$\Delta_P = -\frac{1}{2} \int_0^{\tau_0} d\tau e^{ik\mu(\tau-\tau_0)} e^{-\kappa} \dot{\kappa} [1 - P_2(\mu)] \Pi. \quad (3.1)$$

The visibility function $\dot{\kappa} e^{-\kappa}$ has two peaks; one at recombination and the other due to reionization, so it is convenient to separate the previous integral in two parts:

$$\Delta_P = -\frac{1}{2} [1 - P_2(\mu)] \left(\int_0^{\tau_{\text{ri}}} d\tau e^{ik\mu(\tau-\tau_0)} \dot{\kappa} e^{-\kappa} \Pi + \int_{\tau_{\text{ri}}}^{\tau_0} d\tau e^{ik\mu(\tau-\tau_0)} \dot{\kappa} e^{-\kappa} \Pi \right) \quad (3.2)$$

where τ_{ri} is the conformal time of the start of reionization. The first integral just represents the polarization generated at recombination and can easily be shown to be

$$\Delta_P^{(1)} \equiv -\frac{1}{2} [1 - P_2(\mu)] \int_0^{\tau_{\text{ri}}} d\tau e^{ik\mu(\tau-\tau_0)} \dot{\kappa} e^{-\kappa} \Pi = e^{-\kappa_{\text{ri}}} \Delta_P^{\text{NR}} \quad (3.3)$$

where Δ_P^{NR} is the polarization that would be measured if there was no reionization, as discussed in the previous section. This contribution is damped because only a fraction $\exp(-\kappa_{\text{ri}})$ of the photons that arrive to the observer came directly from recombination without scattering again after reionization.

Let us now consider the new contribution arising from reionization. The polarization source is $\Pi = \Delta_{T2} + \Delta_{P2} + \Delta_{P0}$. Δ_{T2} is large coming from the free streaming of the monopole at recombination, while the polarization terms do not grow after decoupling and are thus negligible to first approximation. Equation (3.2) shows that the new polarization is basically an average of the value of the temperature

quadrupole during the reionization scattering surface. This accounts for all the new features in the polarization power spectrum of Fig. 1.

To understand the origin of these new peaks let us find the amplitude of the temperature quadrupole at the time reionization starts τ_{ri} . The monopole at recombination is approximately given by [4]

$$(\Delta_{T0} + \psi)(\tau_D) = \frac{1}{3} \psi(1 + 3R) \cos(kc_s \tau_D) - R\psi. \quad (3.4)$$

ψ is just the value of the gravitational potential (assumed constant), $R = 3\rho_b/4\rho_\gamma|_{\tau_D} \approx 30\Omega_b h^2$, and $c_s = 1/\sqrt{(1+R)}$ is the photon-baryon sound speed. The quadrupole at τ_{ri} arising from the free streaming of this monopole is simply

$$\Delta_{T2}(\tau_{\text{ri}}) = (\Delta_{T0} + \psi)(\tau_D) j_2[k(\tau_{\text{ri}} - \tau_D)], \quad (3.5)$$

where j_2 is the $l=2$ spherical Bessel function.

The peaks of the previous expression as a function of k will show up in the polarization power spectrum. The first peak of Eq. (3.5) is approximately at the first peak of the Bessel function because $c_s \tau_D \ll (\tau_{\text{ri}} - \tau_D)$. The wave vector for this first peak is approximately given by $k(\tau_{\text{ri}} - \tau_D) \sim 2$, this wave vector translates into an l value as usual according to $l \sim k(\tau_0 - \tau_{\text{ri}})$ and thus the l value for the first is $l \sim 2(\tau_0 - \tau_{\text{ri}})/(\tau_{\text{ri}} - \tau_D) \sim 2\sqrt{z_{\text{ri}}}$. For the case under consideration this means $l \sim 24$ which agrees very well with the first peak in Fig. 3. Only the first peaks appear because the reionization scattering surface is very wide and thus the integrand in Eq. (3.2) for smaller wavelengths oscillates during its width and cancels out after integration. This cancellation makes the new polarization small and thus hidden under the polarization generated at recombination.

The major factor determining the difference in height of these new peaks for different models is the fraction of photons reaching the observer that last scattered after reionization, $1 - \exp(-\kappa_{\text{ri}})$. Thus the ratio of the distances between the observer and reionization to that between the two scattering surfaces determines the positions of the peaks, and the optical depth κ_{ri} their heights.

To further illustrate these points Fig. 3(a) shows the C_{El} spectrum for Λ CDM models with varying optical depths κ_{ri} . The peaks not only vary in height but also in position, as the redshift of reionization has to increase in order to increase κ_{ri} , thus the ratio of distances that determines the position of the peaks gets bigger, as $(\tau_0 - \tau_{\text{ri}})$ increases and $(\tau_{\text{ri}} - \tau_D)$ decreases, driving the peaks to a smaller angle ($l_{\text{peak}} \propto \sqrt{z_{\text{ri}}}$).

Figure 3(b), on the other hand, shows how these peaks vary with the cosmological constant for a fixed reionization redshift $z_{\text{ri}} = 100$. The positions hardly change as both the distance to reionization and the distance between the two scattering surfaces scales approximately in the same way with the matter density (in this calculations the matter density was given by $\Omega_0 = 1 - \Omega_\Lambda$, where Ω_Λ is the energy density due to the cosmological constant). On the other hand, as the distance to a fixed redshift increases with the cosmological constant, the optical depth κ_{ri} increases, and consequently the peaks should get higher. The fact that this is not the case is a consequence of the COBE normalization, models with larger values of the cosmological constant have

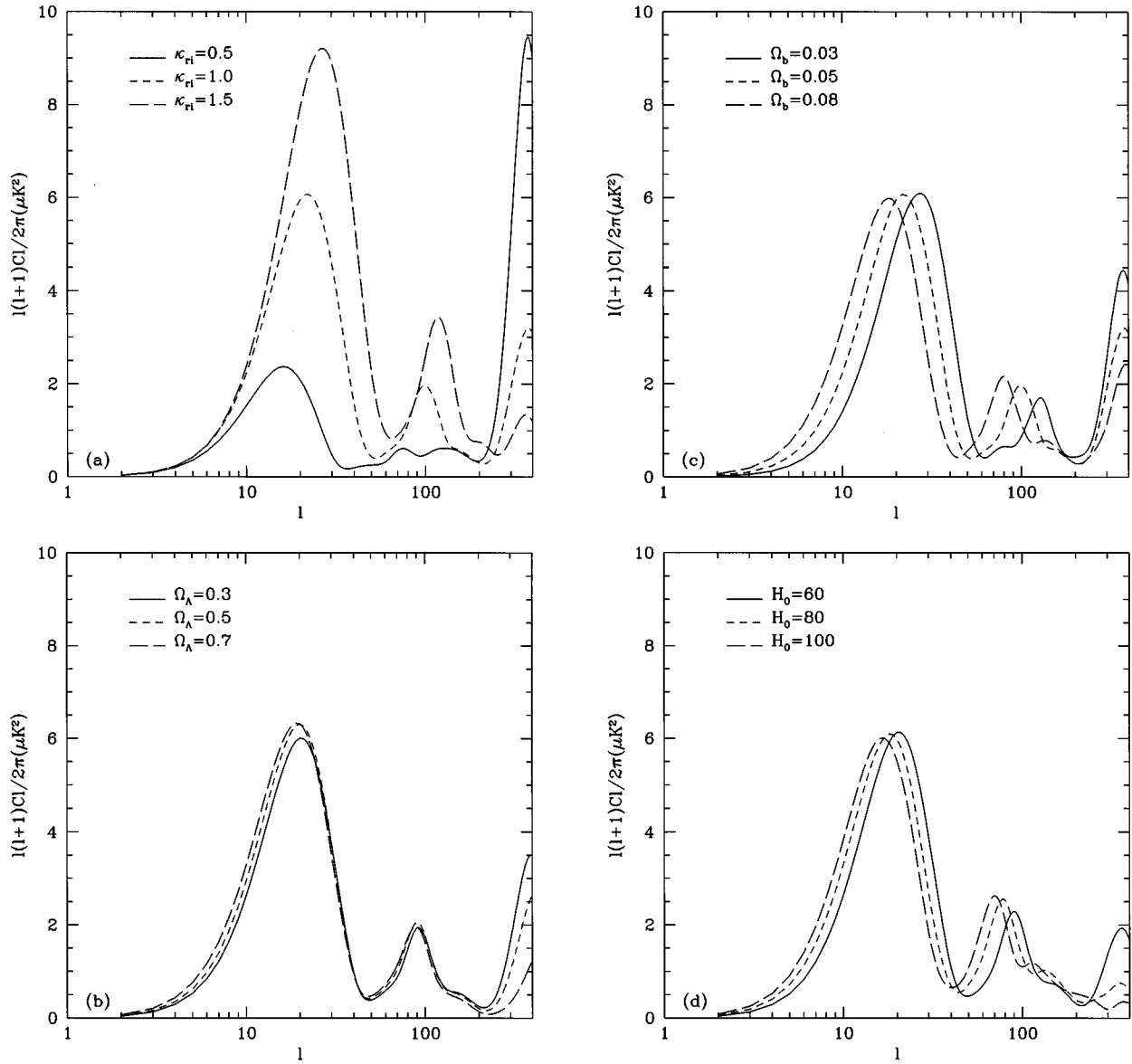


FIG. 3. $l(l+1)C_l/2\pi$ (a) for CDM models with varying $\kappa_{\text{ri}}=0.5, 1.0, 1.5$, and (b) for models with varying cosmological constant $\Omega_\Lambda=0.3, 0.5, 0.7$, and a fixed redshift of reionization $z_{\text{ri}}=100$. Reionized ($\kappa_{\text{ri}}=1.0$) CDM models (c) with varying $\Omega_b=0.3, 0.5, 0.8$, and (d) with different Hubble constants $H_0=60, 80, 100 \text{ km sec}^{-1} \text{ Mpc}^{-1}$. In all cases reionization was assumed to be total ($x_e=1$).

larger additional contributions to the low l temperature anisotropies from the integrated Sachs-Wolfe (ISW) effect while polarization is not affected by the ISW. Thus the changes in the normalization to keep the value of C_{T10} fixed partially compensates the change in the height of the new polarization peaks produced by the larger optical depth.

Figures 3(c) and 3(d) explore the dependence of the polarization power spectrum with the baryon density and the Hubble constant for a fixed optical depth to decoupling, $\kappa_{\text{ri}}=1.0$. The rest of the parameters were kept equal to those of SCDM. The height of the first peak in the spectrum remains nearly constant as it is determined by κ_{ri} which was kept fixed. The fact that the peaks move is simple to understand, the redshift of reionization is given by $(1+z_{\text{ri}}) \approx 100[\kappa_{\text{ri}}(0.5/h)(0.05/\Omega_b)(1/x_e)]^{2/3}$ and so l scales approximately as $l \propto (\kappa_{\text{ri}}/h\Omega_b x_e)^{1/3}$.

In the SCDM model reionization must have occurred extremely early ($z_{\text{ri}} \approx 100$) in order to produce an optical depth

of one; even an optical depth of $\kappa_{\text{ri}}=0.5$ is only obtained for a redshift of $z_{\text{ri}} \approx 60$. But the situation is different for open models or models with a cosmological constant. An approximate scaling for the optical depth valid for $\Omega_0 z_{\text{ri}} \gg 1$ is $\kappa_{\text{ri}} \propto (h\Omega_b x_e / \Omega_0^{1/2})(1+z_{\text{ri}})^{3/2}$, so for example reionization starting at $z_{\text{ri}} \approx 23$ will produce an optical depth $\kappa_{\text{ri}} \approx 0.5$ in a model with $\Omega_0=0.2$, $H_0=70 \text{ km sec}^{-1} \text{ Mpc}^{-1}$ and $\Omega_b=0.1$.

IV. MEASURING POLARIZATION

In this section I discuss the possibility of detecting polarization in the context of the standard theoretical models. I first concentrate in an experiment like the one being built at Brown University and in this case only in the detection of the rms degree of linear polarization and not on the measurement of the correlation function. Then I discuss the prospect of future satellite missions like MAP.

A. The Brown experiment

The Brown experiment will try to measure both Q and U parameters with an expected sensitivity of $1 \mu\text{K}$. The instrument will allow measurements with a 7° FWHM at an early stage and a 1° FWHM afterwards. For concreteness I will just take a Gaussian window function, $W_l = \exp[-(l+0.5)^2 \sigma_\theta^2]$, $\sigma_\theta = \theta/2\sqrt{2\ln 2}$, where θ is the FWHM of the detector in radians. The predicted values for the Stokes parameters were calculated using CMBFAST and the spectra normalized to COBE.

First let us quote the expected rms value of Q for standard CDM with no reionization, $P(7^\circ) = 4.8 \times 10^{-2} \mu\text{K}$ and $P(1^\circ) = 0.77 \mu\text{K}$. These values, specially the large angular scale one, are extremely small and thus very difficult to detect. This is the reason why the reionized scenarios are the most promising to detect polarization.

Reionization will not only change the polarization power spectrum but also the temperature one, and in some cases it may wash away the Doppler peaks completely. But there is some degree of confusion between the different parameters determining the CMB spectra, for example a reionization with a moderate optical depth will decrease the amplitude of the Doppler peaks but this effect may be compensated by changing the spectral index [3]. In fact only an optical depth in the 10–20% range seem detectable from temperature maps alone [27]. Figure 4 shows both polarization and temperature power spectra for SCDM with a spectral index $n=1$ and a reionized model with $\kappa_{\text{ri}}=0.5$ but a spectral index $n=1.2$. The difference in the anisotropy power spectrum is not so large, while the polarization spectra are very different. The rms P values in this reionized case are $P(7^\circ) = 1.2 \mu\text{K}$ and $P(1^\circ) = 1.8 \mu\text{K}$. For the large angular scale experiment the difference with SCDM is more than two orders of magnitude and in the one degree case is more than a factor of two. Thus a polarization measurement would easily distinguish between the two scenarios.

Figure 5 shows the rms value of P as a function of κ_{ri} , the major parameter determining the amplitude of the polarization perturbation. $P(7^\circ)$ only exceeds $1 \mu\text{K}$ level for $\kappa_{\text{ri}} \geq 0.5$ but saturates quickly near $1.8 \mu\text{K}$. On the other hand $P(1^\circ)$ quickly raises above the $1 \mu\text{K}$ and reaches $3.2 \mu\text{K}$ for an optical depth of two. This means that even a negative detection at the $1 \mu\text{K}$ level for the one degree experiment is enough to rule out some models, those with optical $\kappa_{\text{ri}} \geq 0.3$.

Parameters other than κ_{ri} do not make much difference in the height of the peaks. Table I explores the dependence of $P(7^\circ)$ and $P(1^\circ)$ with different cosmological parameters for a fixed $\kappa_{\text{ri}}=1.0$. Although the height of the peaks remains almost constant these models slight shifts in their location change the predicted P . The 7° rms linear polarization is more sensitive to the position of the first peak. The 1° experiment has the largest chance of putting interesting constraints on a possible reionization as the expected signal is greater, because it is sensitive to all the power in the new peaks of the polarization power spectrum. A correlation analysis between the polarization in the forty pixels that the experiment will measure may help improve the above limits.

B. Future satellite missions

There are now two planned satellite missions to map the microwave sky MAP [17] and COBRAS/SAMBA [18]

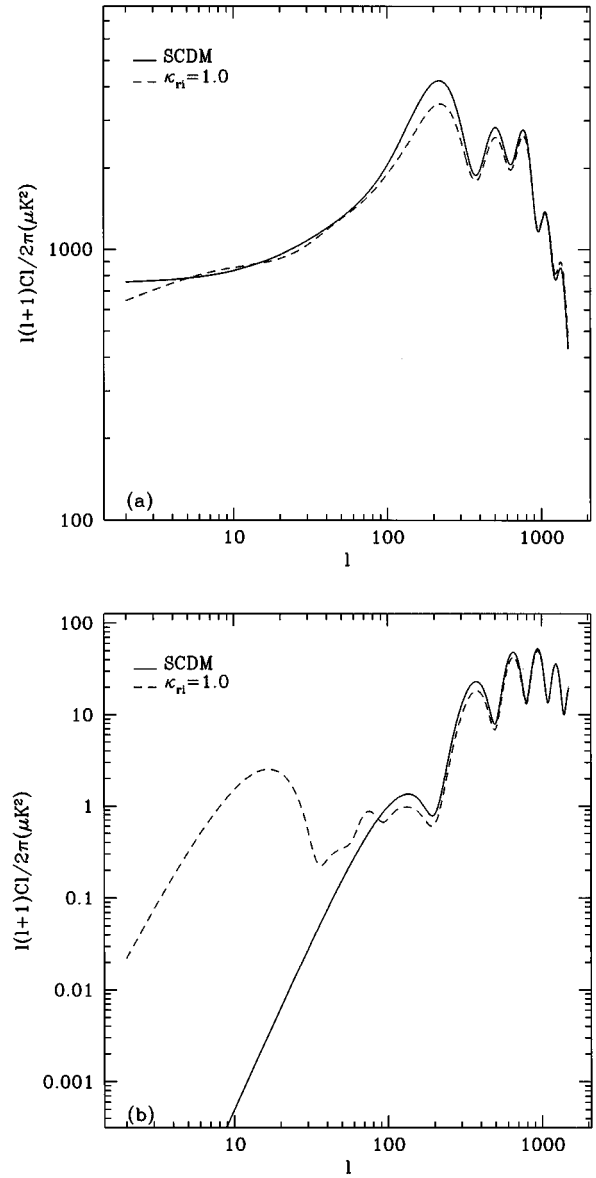


FIG. 4. $l(l+1)C_l/2\pi$ for both temperature (a) and polarization (b) for standard CDM and a model where the optical depth to recombination is $\kappa_{\text{ri}}=0.5$ and a spectral index $n=1.2$.

which will have polarization information. Temperature information alone cannot put very stringent limits on the epoch of reionization [27]. With noise levels realistic for MAP only $\kappa_{\text{ri}} \sim 0.1$ could be detected. The problem is that the dominant effect of reionization on the temperature on small angular scales is a suppression equivalent to a decrease in the amplitude of the primordial perturbations. This degeneracy is broken on large scales as reionization does not significantly affect the amplitude on these scales, but here cosmic variance precludes very accurate determinations. One may hope to improve the accuracy in the estimation of the optical depth by measuring the new peaks in the polarization power spectra.

Figure 6 illustrates these points. In panel (a) the spectra for a COBE normalized SCDM and a reionized model with $\kappa_{\text{ri}}=0.1$ are plotted. The reionized model has been normalized in such a way as to minimize the χ^2 difference between the two. I have assumed for simplicity that each C_l is Gauss-

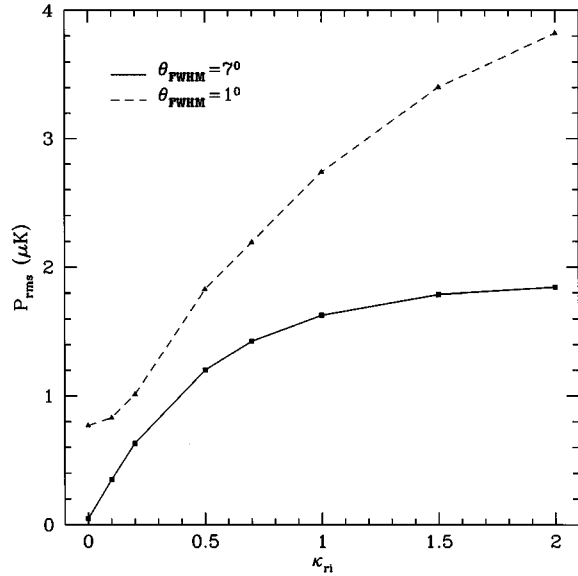


FIG. 5. Polarization rms fluctuations (μK) as a function of the optical depth, κ_{ri} for a 7° and 1° FWHM experiments.

ian distributed with a variance given by [27]

$$\sigma_l = \sqrt{\frac{2}{2l+1}} [C_l + w^{-1} \exp(l^2 \sigma_b^2)] \quad (4.1)$$

where $\sigma_b^2 = 7.42 \times 10^{-3} (\theta_{\text{FWHM}}/1^\circ)$ for a Gaussian beam and w^{-1} is a pixel size independent measure of experimental noise. Values corresponding to the MAP mission were used ($w^{-1} = 4.2 \times 10^{-15}$ and $\theta_{\text{FWHM}} = 0.29^\circ$).

Figure 6(b) shows the polarization power spectra for the same models, the difference in the large scale polarization

TABLE I. Degree of linear polarization in μK SCDM (first row) and several other models all with $\kappa_{\text{ri}} = 1.0$. The value of the cosmological constant is such that all the above models are flat, $\Omega_{\text{total}} = 1.0$. H_0 is the Hubble constant in $\text{km sec}^{-1} \text{Mpc}^{-1}$.

| Ω_0 | Ω_b | H_0 | $P(7^\circ)$ | $P(1^\circ)$ |
|------------|------------|-------|-----------------------|--------------|
| 1.0 | 0.05 | 50 | 4.81×10^{-2} | 0.642 |
| 0.7 | 0.05 | 50 | 1.62 | 2.25 |
| 0.5 | 0.05 | 50 | 1.67 | 2.50 |
| 0.3 | 0.05 | 50 | 1.62 | 2.25 |
| 1.0 | 0.03 | 50 | 1.40 | 2.67 |
| 1.0 | 0.08 | 50 | 1.83 | 2.79 |
| 1.0 | 0.10 | 50 | 1.91 | 2.80 |
| 1.0 | 0.05 | 60 | 1.72 | 2.79 |
| 1.0 | 0.05 | 80 | 1.84 | 2.85 |
| 1.0 | 0.05 | 100 | 1.92 | 2.88 |

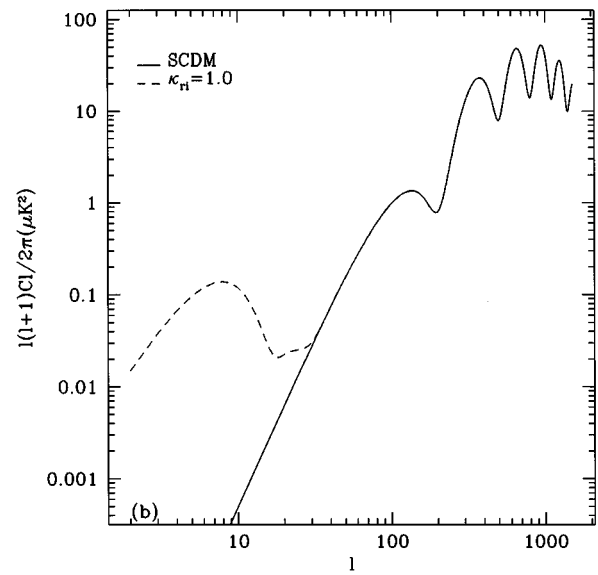
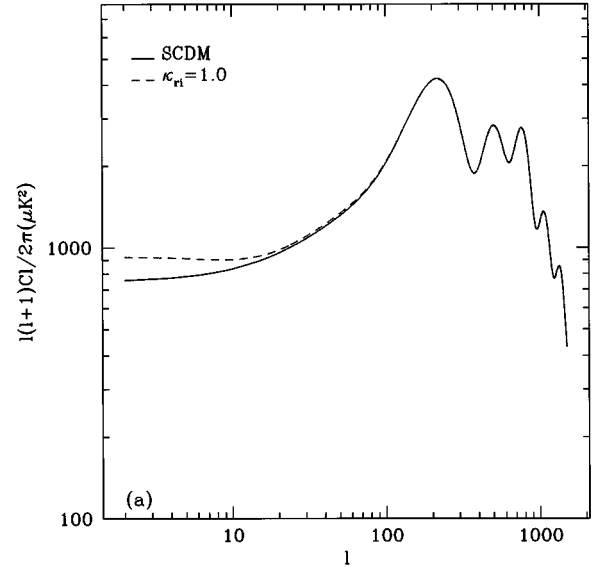


FIG. 6. Temperature and polarization power spectra for a COBE normalized SCDM and a reionized model with $\kappa_{\text{ri}} = 0.1$.

greatly exceeds the cosmic variance. The value of the multipoles C_{El} at the reionization peak in this model are $C_{\text{El}} \sim (0.12 \mu\text{K})^2$, to be compared to a noise in each a_{lm} of roughly $0.14 \mu\text{K}$ for polarization [28] in the case of the MAP mission. This makes the possibility of using polarization to further constrain the optical depth very interesting. It is also worth noting that the noise levels of COBRAS/SAMBA detectors is much lower, and so better sensitivities should be expected in this case.

V. CONCLUSIONS

The polarization of the microwave background is very sensitive to the ionization history of the universe and an early reionization can greatly enhance it. I have discussed in detail the physics behind the generation of polarization in reionized scenarios and the appearance of new peaks in the polarization power spectrum. I have identified the major parameters determining the location of these peaks, the ratio of

distances between the observer and the reionization scattering surface to that between reionization and recombination. The height of the peaks is mainly a function of κ_{ri} , the optical depth to recombination.

An early reionization with an optical depth $\kappa_{\text{ri}} \geq 0.5$ can take large and intermediate angular scale polarization to the μK level, detectable in the near future by the Brown Experiment. Polarization may help resolve some of the ‘‘confusion’’ that can arise when determining cosmological param-

eters using CMB. In particular it may help detect levels of reionization below the $\kappa_{\text{ri}} \sim 0.1$ that can be obtained with temperature maps alone.

ACKNOWLEDGMENTS

I am very grateful to Uroš Seljak for his encouragement and many useful discussions. I would also want to thank Ed Bertschinger and David Spergel for reading the manuscript.

-
- [1] J. R. Bond, in *Cosmology and Large Scale Structure*, edited by R. Schaeffer *et al.* (Elsevier Science, Netherlands, 1996).
 - [2] D. Scott, J. Silk, and M. White, *Science* **268**, 829 (1995).
 - [3] J. R. Bond *et al.*, *Phys. Rev. Lett.* **72**, 13 (1994).
 - [4] W. Hu, N. Sugiyama, and J. Silk, *Nature* (London) (to be published).
 - [5] U. Seljak, *Astrophys. J.* **435**, L87 (1994).
 - [6] J. R. Bond and G. Efstathiou, *Mon. Not. R. Astron. Soc.* **226**, 655 (1987).
 - [7] M. Zaldarriaga and D. Harari, *Phys. Rev. D* **52**, 3276 (1995).
 - [8] R. Crittenden, R. L. Davis, D. Coulson, and N. Turok, *Phys. Rev. D* **52**, 5402 (1995).
 - [9] K. L. Ng and K. W. Ng, *Astrophys. J.* **456**, 413 (1996).
 - [10] D. Harari and M. Zaldarriaga, *Phys. Lett. B* **319**, 96 (1993).
 - [11] R. Crittenden, D. Coulson, and N. Turok, *Phys. Rev. D* **52**, 5402 (1995).
 - [12] A. Loeb and A. Kosowsky, Report No. astro-ph/9601055, 1996 (unpublished).
 - [13] A. A. Penzias and R. W. Wilson, *Astrophys. J.* **142**, 419 (1965).
 - [14] G. P. Nanos, *Astrophys. J.* **232**, 341 (1979).
 - [15] N. Caderni *et al.*, *Phys. Rev. D* **17**, 1908 (1978).
 - [16] P. M. Lubin and G. F. Smoot, *Astrophys. J.* **245**, 1 (1981).
 - [17] Visit the MAP home page at <http://map.gsfc.nasa.gov>
 - [18] Visit the COBRAS/SAMBAS home page at <http://astro.estec.esa.nl/SA-general/Projects/Cobras/cobras.html>
 - [19] J. R. Bond and G. Efstathiou, *Astrophys. J.* **285**, L45 (1984).
 - [20] R. A. Frewin, A. G. Polnarev, and P. Coles, *Mon. Not. R. Astron. Soc.* **266**, L21 (1994).
 - [21] U. Seljak and M. Zaldarriaga, *Astrophys. J.* **469**, 437 (1996).
 - [22] A. Kosowsky, *Ann. Phys. (N.Y.)* **246**, 49 (1996).
 - [23] M. Zaldarriaga and U. Seljak, Report No. astro-ph/9609170, 1996 (unpublished).
 - [24] E. F. Bunn and M. White, Report No. astro-ph/9602019, 1996 (unpublished).
 - [25] W. Hu and N. Sugiyama, *Astrophys. J.* **436**, 456 (1995).
 - [26] W. Hu and N. Sugiyama, *Phys. Rev. D* **51**, 2599 (1995).
 - [27] G. Jungman, M. Kamionkowski, A. Kosowsky, and D. N. Spergel, *Phys. Rev. Lett.* **76**, 1007 (1996). See also Report No. astro-ph/9605147 for a discussion in terms of the parameters of the MAP and COBRAS/SAMBAS planned experiments.
 - [28] D. Spergel (private communication).